

Long Short-Term Memory Neural Network assisted Peak to Average Power Ratio Reduction for Underwater Acoustic Orthogonal Frequency Division Multiplexing Communication

Waleed Raza¹, Xuefei Ma^{2*}, Houbing Song^{3*}, Amir Ali⁴, Habib Zubairi⁴, and Kamal Acharya¹

¹Department of Electrical and Computer Engineering, Embry Riddle Aeronautical University, Daytona Beach, FL 32114 USA

[e-mail: razaw@my.erau.edu, acharyk2@my.erau.edu]

²College of Information and Communication Engineering, Harbin Engineering University, Harbin 150001, China

[e-mail: maxuefei@edu.cn]

³Department of Information Systems, University of Maryland, Baltimore County Baltimore, MD 21250 USA

[e-mail: songh@umbc.edu]

⁴College of Underwater Acoustic Engineering, Harbin Engineering University, Harbin 150001, China

* Corresponding author: Xuefei Ma, Houbing Song

Received November 7, 2022; revised December 7, 2022; revised January 2, 2023; accepted January 7, 2023; published January 31, 2023

Abstract

The underwater acoustic wireless communication networks are generally formed by the different autonomous underwater acoustic vehicles, and transceivers interconnected to the bottom of the ocean with battery deployed modems. Orthogonal frequency division multiplexing (OFDM) has become the most popular modulation technique in underwater acoustic communication due to its high data transmission and robustness over other symmetrical modulation techniques. To maintain the operability of underwater acoustic communication networks, the power consumption of battery-operated transceivers becomes a vital necessity to be minimized. The OFDM technology has a major lack of peak to average power ratio (PAPR) which results in the consumption of more power, creating non-linear distortion and increasing the bit error rate (BER). To overcome this situation, we have contributed our symmetry research into three dimensions. Firstly, we propose a machine learning-based underwater acoustic communication system through long short-term memory neural network (LSTM-NN). Secondly, the proposed LSTM-NN reduces the PAPR and makes the system reliable and efficient, which turns into a better performance of BER. Finally, the simulation and water tank experimental data results are executed which proves that the LSTM-NN is the best solution for mitigating the PAPR with non-linear distortion and complexity in the overall communication system.

Keywords: underwater acoustic communication; orthogonal frequency divisional multiplexing; long short-time memory neural network; machine learning; PAPR

1. Introduction

The underwater acoustic communication networks (UACN) are formed for end-to-end communication for the exploration of the ocean and many other applications. For security and defense purposes, uncountable applications have been found, where UACN has played vital roles. Some applications of end-to-end communication related to non-military are oceanographic data collection, pollution monitoring, offshore exploration, natural disaster prevention, assisted navigation, and tactical surveillance, while also have many applications in military purposes communication, where secure, reliable, and fast responsive communication networks are preferred [1-3]. The operations of the navy are monitored based on highly responsive UACN during the war zone.

Moreover, the commercial development of UACN increases as the need increases in many real-time applications such as pollution monitoring of streams, seismic imaging, lakes, ocean bays, drinking water reservoirs, local ponds, the biological behavior of different animals in different oceans, and can also be used where leakage of oil detection is required [4, 5]. Underwater acoustic communication (UAC) is considered as the key tool of UACN, so the sparse network topology and wireless communication are preferable for the exchange of massive information underwater, instead of deploying costly wired networks [6].

Different symmetrical communication media have different behavior in underwater and can propagate up to a certain range. The radio frequencies can propagate several meters, optical waves can propagate up to tens of meters, and on the other hand magnetically coupled communication has been introduced recently for short-range UAC communication in the literature [7, 8]. Looking at the behavior of all these communication media, the acoustic wave can propagate over a wide range i.e., up to 40 km with minimal loss. So, the acoustic wave is a better choice in underwater communication networks and is the key technology to realize the UACN.

The orthogonal frequency division multiplexing (OFDM) has achieved huge importance in the terrestrial wireless communication system, now it is being shifted towards UACN [9]. The communication networks in the underwater acoustic medium are different from terrestrial radio-based networks due to huge propagation delays, high transmit energy, low bandwidth, and various multipath effects [10, 11]. The propagation speed of the acoustic signal in the water depends on different factors, i.e., salinity, temperature, and pressure, which is about five orders less than radio signals in magnitude [3, 12].

For wireless communication in underwater acoustic medium, OFDM technology is implemented, keeping in mind about time-varying nature of the acoustic channel. When the communication is established, it faces multipath propagation and Doppler shift, which makes the communication system more challenging [6, 13, 14]. Even though looking at several advantages of OFDM i.e. high data rate and better bandwidth efficiency it also undergoes some drawbacks such as peak to average power ratio (PAPR) and carrier frequency offset [15, 16]. When high peaks resulting during communication are allowed to pass through the non-linear

region of the power amplifier (PA), then it will distort the communication system. The overall efficiency of the system is reduced, and complexity becomes very high for analog-to-digital converters (ADC) and digital-to-analog converters (DAC) [15, 17, 18]. Particularly, the energy efficiency (EE) is decreased which is due to high PAPR in battery-powered modems in the UACN. Also, the performance of the signal-to-quantization-noise ratio (SQNR) is affected.

To overcome this situation, large power back-off, high-power amplifiers (HPA), and linear converters are required [19-21]. After approaching these requirements, the hardware becomes much more costly, and the system will be more complex. The cost is also the main factor in designing the hardware components. So the OFDM system must be less complex with a lower PAPR [22]. In this paper, the novel long short-term memory neural network (LSTM-NN) based OFDM system is proposed. The PAPR of an OFDM signal is mitigated using a modern machine learning (ML) algorithm named as LSTM-NN algorithm, which is the best-fit process for the mitigation of PAPR. The data is passed through a multipath fading UAC channel. Then, at the receiver side, the OFDM symbols are received by using 16-quadrature amplitude modulation (16-QAM) with successful decoding and efficient performance of bit error rate (BER). The simulation results show that the proposed LSTM-NN has better performance in terms of PAPR reduction compared with the traditional OFDM system.

1.1 Literature Overview

The ML is an efficient tool to solve many complex problems like object tracking, recognition of voice, and detection of objects. Also, it has vast applications in computer vision and natural language processing. Artificial intelligence (AI) has led the basis in digital signal processing, and the subcategories of AI such as deep learning (DL) and ML will be the main part of the internet of things (IoT) and smart cities for the future generation of heterogeneous networks [25, 26]. In this article, we aim to implement ML and DL based methods in underwater acoustic OFDM communication. Therefore, this subsection is dedicated to a brief survey of AI-based literature and research.

In 2019, Zhang et al. introduced a deep learning-based UAC system [27]. In this work, the focus was mainly on designing the DL-based OFDM receiver. He trained the deep neural network (DNN) in labeled and unlabeled data, after using the acoustic propagation model and giving sound speed profiles to train the DNN based OFDM receiver. The ML based OFDM communication system was introduced in [28], which predicts and estimates impulsive noise. At the receiver, the ML classifiers were trained with different impulsive noise statistics which predict the discrete Fourier transforms (DFT) samples of the OFDM system, containing impulsive noise. Hao et al. estimated the channel using deep learning technology in [29], this method identifies the channel distortion using a DL model based on channel characteristics. The same work was presented in [30], this scheme was named a de-noising autoencoder for an OFDM communication system based on a neural network. The noise of the channel is reduced, and it estimates the channel transfer function by using the autoencoder of the ML.

Mingshan et al. proposed a neural network-assisted active constellation expansion method (NN-ACE) which is also based on an autoencoder for mitigating the PAPR [31]. An autoencoder learns the extension vector of ACE which keeps the signal power low. Furthermore, in the loss function, a technique was given to maintain the PAPR reduction and power increment by a weight factor. In [25] the authors presented research that was based on the autoencoder architecture of deep learning and the method was named PAPR reducing network (PRNet). In the proposed PRNet method, a deep learning network was employed which determines the constellation and demapping of each subcarrier adaptively. Also, it reduces both the PAPR and the BER jointly. The tone reservation based on deep learning (DL-

TR) was proposed by Lanping et al. which is also operated for the reduction of PAPR in OFDM signals [32]. Besides this, several other PAPR reduction algorithms were proposed in the literature such as genetic algorithm (GA), particle swarm optimization (PSO) with selective mapping and partial transmit sequences at the cost of complexity [33-38]. After then several DL and ML based approaches were proposed in [39-42]. Whereas this article mainly focuses on implementing the LSTM-NN for the OFDM system and is proposed for the first time according to our best knowledge. In this model, the novel LSTM-NN assisted OFDM system is introduced. Secondly, the PAPR of an OFDM signal is reduced using a modern ML algorithm named LSTM-NN algorithm. Then the simulation is performed, considering real data transmission to obtain optimal performance of the overall system with lesser complexity and efficient performance of BER.

2. System Model

The underwater acoustic OFDM communication system comprises the single transducer and single receiver denoted as N_t , N_r respectively. The time duration of each OFDM block in the system is expressed as $T' = T + T_g$, in the expression, the OFDM symbol is shown as T , and the guard interval is given as T_g . Here, $1/T$ is subcarrier spacing [43]. At frequency f_k , the k th subcarrier is expressed as:

$$f_k = f_c + \frac{k}{T}, \quad k = \frac{K}{2}, \dots, K/2 - 1 \quad (1)$$

In equation (1) the carrier frequency is given as f_c , and the number of subcarriers is expressed as K . Hence, the bandwidth is $B = K/T$. We suppose the encoded information symbols as $S_u[k]$ also the pulse shape filter is shown as $g(t)$. Finally, the signal which is transmitted by u th the transducer is illustrated as:

$$\tilde{x}_u(t) = 2 \operatorname{Re} \left\{ \left[\sum_{k \in S_A} S_u[k] e^{j2\pi \frac{k}{T} t} g(t) \right] e^{j2\pi f_c t} \right\}, \quad t \in [0, T'] \quad (2)$$

We assume (v, u) th, transducer and hydrophone pair, the multipath channel is comprised of $P_{v,u}$ several discrete paths, then the impulse response of the channel is expressed as:

$$h_{v,u}(\tau, t) = \sum_{p=1}^{P_{v,u}} A_{v,u,p} \delta(\tau - (\tau_{v,u,p} - a_{v,u,p} t)) \quad (3)$$

Here, the amplitude is given as $A_{v,u,p}$ and $\tau_{v,u,p}$ denotes the delay of p th the path of (v, u) th the transducer and hydrophone pair also including the Doppler scaling factor $a_{v,u,p}$. In equation 4, we have illustrated the OFDM system model in the UAC which is different from the terrestrial wireless OFDM communication system by giving the unique underwater acoustic channel, which has severe multipath effects and Doppler effects [44-46]. In the end, the passband signal at the v th receiver after adding noise $n_v(t)$ is given by

$$\tilde{y}_v(t) = \sum_{u=1}^{N_t} \sum_{p=1}^{P_{v,u}} A_{v,u,p} \tilde{x}_u((1 + a_{v,u,p})t - \tau_{v,u,p}) + \tilde{n}_v(t) \quad (4)$$

Fig. 1 explains the basic block diagram of the underwater acoustic OFDM system with the proposed LSTM-NN. In the OFDM systems, the input binary sequence is the first baseband modulated using binary phase-shift keying (BPSK), quadrature phase-shift keying (QPSK),

and quadrature amplitude modulation (QAM), then the data is interleaved and finally modulated utilizing OFDM which is to be transmitted through the channel. Further, it includes the addition of pilots, reduction of PAPR with the proposed LSTM-NN algorithm, inverse fast Fourier transform (IFFT), and cyclic prefix addition. On the receiver side, channel estimation and equalization are performed, which is regarded as an intricate job. Finally, it is demodulated, de-interleaved, and decoded by employing LSTM-NN after the fast Fourier transform and performing channel estimation and equalization.

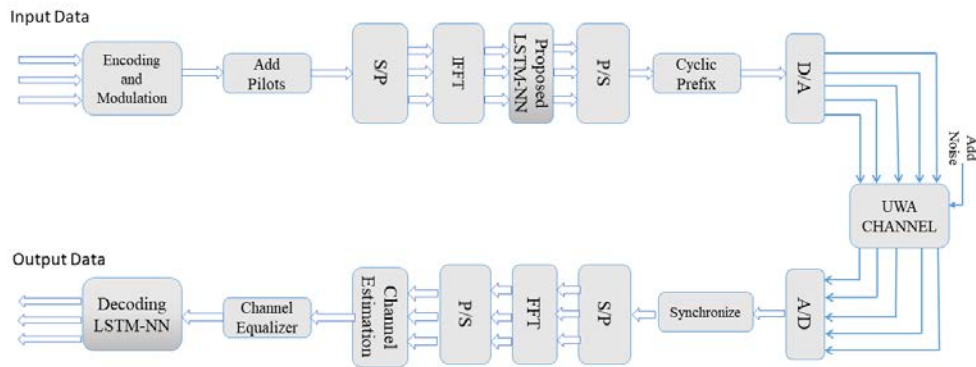


Fig. 1. The framework/system model of an underwater acoustic OFDM communication system with LSTM-NN

2.1 Peak to Average Power Ratio

The value of peak power is always larger than the average power in an OFDM signal because a large number of subcarriers are added coherently resulting in high PAPR [47, 48]. In the UAC system, PAPR has high significance over the transmitted signal because the power efficiency is affected by PAPR. Also, the PAPR directly affects the performance of the PA. When the value of PAPR is high, the peak signals are shifted towards the nonlinear region of the PA, hence power efficiency is decreased. The inter-symbol interference (ISI), as well as ICI, is due to nonlinearity among OFDM signals. A continuous time-domain signal in terms of PAPR can be given in the following equation,

$$PAPR = \frac{\max_t |x(t)|^2}{E_t [|x(t)|^2]} \quad (5)$$

The time-domain signal can be given mathematically as:

$$PAPR = \frac{\max_n |x(n)|^2}{E_n [|x(n)|^2]} \quad (6)$$

To check the performance of PAPR in OFDM transmitted signals the complementary commutative distribution function (CCDF) of PAPR is used which exhibits the performance of PAPR reduction schemes. It can be given for a specific level $PAPR_0$ as,

$$CCDF_{PAPR} = P_r(PAPR > PAPR_0) \quad (7)$$

For the Gaussian time-domain signal, it is illustrated as,

$$CCDF_{PAPR} = 1 - (1 - e^{-PAPR_0})^\kappa \quad (8)$$

In the above equation, κ expresses the number of subcarriers.

3. Proposed Method with Long Short-term Memory Neural Network (LSTM-NN) and Training the Data

We have proposed an underwater acoustic OFDM communication system to reduce the PAPR and nonlinear distortion. The distortion which is caused by PA increases the BER and degrades the performance of the communication system. To resolve this issue, we need to train the data using the LSTM-NN at the transmitting end in such a way that it should learn quickly and have some memory. The input signals are fed to the transmitter end where high energized peaks appear, the proposed algorithm minimizes those high peaks. And, before making PA in a non-linear region, the training of data is needed at the transmitter side so that a receiver may not experience the BER problem resulting in loss of information. Several PAPR mitigation methods based on DNN have been proposed in the literature. But here, we have employed the recurrent neural network (RNN) based LSTM-NN. To understand LSTM-NN, we must know about RNN. The RNN is widely used to solve many problems and it has many applications such as object tracking, recognition of voice, and detection of objects. RNNs are different from simple neural networks as RNNs collect information and remember it for the time being. Also, RNNs are independent of weights and input information. The RNN has much importance with optimum efficiency, but these networks can work up to fewer steps (up to 5 to 10 steps). For further increments in steps i.e., hidden layers, that can be handled by another method which is LSTM-NN (can handle up to 1000 steps).

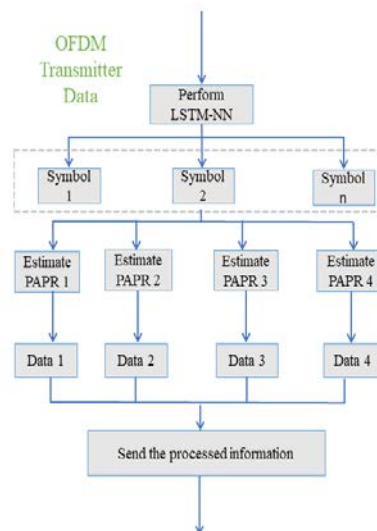


Fig. 2. Flowchart of proposed LSTM-NN

Fig. 2 shows the flowchart of the proposed algorithm which reduces the PAPR by selecting the data which has the lowest PAPR value in the system. Firstly, from the OFDM symbols, it estimates the PAPR and then selects those data for transmission which does not have high PAPR and distortion. The next sub-section describes the overall mechanism of the proposed algorithm and principal derivation.

3.1 Connection Temporal Classification

In the learning process, DNN classifies frame levels in finding PAPR during communication, in the same way, RNN also follows the same rule. In which each frame is being targeted to be learned, the alignment determines the separating line between higher peaks and lower peaks, which is done by the Hidden Markov Model (HMM). **Table 1** illustrates the training and performance of the state of the trained model with $77400 \times 6^*$ the data set, which takes a little more time and iterations to train the model that is less than or equal to 74.59 seconds. The HMM is employed and the MSE is 0.00138 at 132 iterations with random data.

Table 1. Training the Data

Training Model	Data Needed	Time of Training	Fit Goodness
Hidden Markov Model	$77400 \times 6^*$ Number of OFDM symbols = 900	≤ 74.59 sec.	MSE: .00138 at 132 iterations Data Division Random

The training model of HMM performs well but does not provide ideal performance where secure and reliable communication is required. For that connectionist temporal classification (CTC) is used to perform such operations [49], which doesn't require the alignments for the classification of input data and targeted data in the learning process. There is only one separated unit for each part, i.e., the higher peaks unit and lower peaks unit. And there is also an 'Empty' unit added, referred to as no peak's occurrence. The empty unit differentiates the higher peaks and lower peaks in the proposed system. The probability of an empty unit with indexing k in the amount of time t can be given as:

$$P_r(k, t | x) = \frac{\exp(y_t^k)}{\sum_{k'} \exp(y_t^{k'})} \quad (9)$$

Where x is the input, y_t^k is the element of the output, and a is the alignment of CTC at the length T of mentioned units i.e. units with peaks and including empty units. So, the probability of a can be defined as the product of the occurrence of probabilities at each time step,

$$P_r(a | x) = \prod_{t=1}^T \Pr(a_t, t | x) \quad (10)$$

There are so many high peaks that occur, and we have separated them from an empty unit in which high peaks don't occur. After this process we add the higher peaks, so the probability of high PAPR at the output can be given as,

$$P_r(y/x) = \sum_{a \in B^{-1}(y)} \Pr(a/x) \quad (11)$$

As we don't know the exact position of higher peaks for that we perform a summation operation then those places will be stored in the memory of LSTM-NN. Afterward, the model

is trained using a CTC function with targeted data y^* such as

$$CTC(x) = -\log \Pr(y^*/x) \quad (12)$$

3.2 Network Architecture

The input sequence of the RNN network is denoted as $x = (x_1, \dots, x_T)$, the hidden layer with $h = (h_1, \dots, h_T)$, and an output layer sequence is $y = (y_1, \dots, y_T)$ by iterating the following equations from $t=1$ to T :

$$h_t = H(W_{ih}x_t + W_{hh}h_{t-1} + b_h) \quad (13)$$

$$y_t = W_{ho}h_t + b_o \quad (14)$$

Where W_{ih} are the matrices of weight belonging to the hidden layer, b_h is the bias vector in the hidden layer, and H is the activation function. In [50] Hochreiter & Schmidhuber built memory cells for purpose of storing the previous data for a long range of length. H can be illustrated in the following functions,

$$i_t = \sigma(W_{xi}x_t + W_{hi}h_{t-1} + W_{ci}c_{t-1} + b_i) \quad (15)$$

$$f_t = \sigma(W_{xf}x_t + W_{hf}h_{t-1} + W_{cf}c_{t-1} + b_f) \quad (16)$$

$$c_t = f_t c_{t-1} + i_t \tanh(W_{xc}x_t + W_{hc}h_{t-1} + b_c) \quad (17)$$

$$o_t = \sigma(W_{xo}x_t + W_{ho}h_{t-1} + W_{co}c_t + b_o) \quad (18)$$

$$h_t = o_t \tanh(c_t) \quad (19)$$

The sigmoid function is denoted by σ , while other variables for defining input gate, output gate, forget gate, and vectors for cell activation are given as i , f , o and c respectively.

These variables have size as a hidden vector h . We also have assigned the subscripts to the weight matrix, for example W_{hi} representing an output hidden matrix, in W_{xo} represents the output-input gate matrix. The noticeable point is that in the cell vector, the m element will only accept the input from the m while declining the bias vectors because gate-cell W_{ci} matrices are always diagonal to each other. The missing function by previously used RNN is the use of only back context and is also known as unidirectional, on other hand finding PAPR in a hydro-acoustic medium requires a bi-directional method known as the bidirectional recurrent neural network (BRNN). In which two hidden layers are placed separately for the processing of the data. In given Fig. 3 and Fig. 4, x_t shows the input and y_t is the output, whereas \vec{h} is the sequence computed by BRNN, and the arrow shows the forward direction, and \overleftarrow{h} in the backward direction. By continuously repeating the process in a backward $t=T$ to 1 and forward $t=1$ to T direction, the output is updated and is as follows,

$$\vec{h}_t = H(W_{x\vec{h}}x_t + W_{h\vec{h}}\vec{h}_{t-1} + b_{\vec{h}}) \quad (20)$$

$$\overleftarrow{h}_t = H(W_{x\overleftarrow{h}}x_t + W_{h\overleftarrow{h}}\overleftarrow{h}_{t+1} + b_{\overleftarrow{h}}) \quad (21)$$

For long-range and operating input in both directions, BRNN and LSTM can be added. The

deep architectural design has made the hybrid systems advanced, which can represent the information at a much higher level.

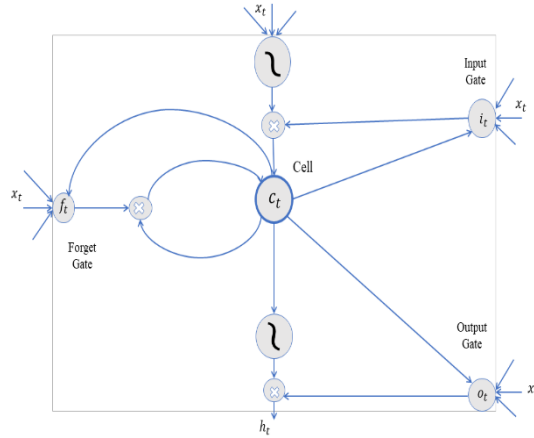


Fig. 3. The memory cell of Long-short Term neural network

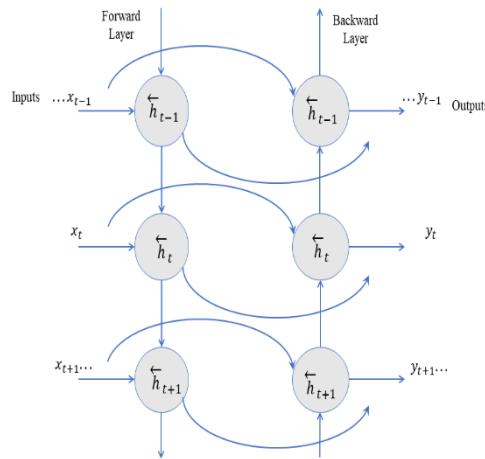


Fig. 4. Bidirectional Recurrent Neural Network.

4. Energy Efficiency Model

The overall EE model is derived for the proposed model in this subsection. To check the performance, we describe the EE metric, which can be expressed as

$$EE = SE / P_r \tag{22}$$

Here, SE represents the obtainable rate which is in bps / hz and P_r is the consumption of related power. For the easier implementation of the system, we are only concerned with the power consumption of PA. For instance, P_{pa} and the IFFT computation for VLSI power consumption we denote P_i , in the end, P_r can be further evaluated into the following two parts:

$$P_r = P_{pa} + P_i \tag{23}$$

There are also other components of power consumption that may affect the performance of EE. While some power components do not have too much influence on EE in the proposed system and the traditional OFDM systems.

The relationship of P_{tx} (transmitted power), and P_{pa} is further illustrated as

$$P_{tx} = \eta P_{pa}, \quad (24)$$

Here η defines the efficiency of PA, which mainly depends upon the type of PA i.e., A, B, C, and AB, etc. Using a different type of PA may affect efficiency, while the logical design of the proposed method is not affected, such as the efficiency of PA class B. Henceforth, η can be given as,

$$\eta(\%) = \frac{\pi}{4p} \times 100, \quad (25)$$

In equation 25, the square root of input back-off (IBO) is given as p . The IBO is defined as the ratio of input power P_{max} (saturation power) of PA and average power P_{ave} . And it can be expressed as follows:

$$IBO(dB) = 10 \log_{10} \left(\frac{P_{max}}{P_{ave}} \right) \quad (26)$$

If the IBO is increased, the distortion can also be minimized, it also reduces the power efficiency. The value of η depends upon the PAPR and the PAPR is dependent on the number of subcarriers and bandwidth. For calculation of P_i it is necessary to explain Gflop (Giga Floating point operation/second) for the IFFT and it can be shown as

$$\zeta(Gflop) = \frac{(T_u B)}{T_s} \cdot \log_2(T_u B), \quad (27)$$

Where T_u illustrates the guard interval (GI) and T_s shows the symbol duration. At present, we will derive the SE to obtain the EE derivation in equation (22). Hence at the receiver side, the signal can be illustrated as:

$$y(n) = \sqrt{p}h(n)\hat{x}(n) + w(n) \quad (28)$$

$$y(n) = \sqrt{p}h(n)\alpha.x(n) + \sqrt{p}h(n)d(n) + w(n) \quad (29)$$

Here, p shows the received power, the additive white Gaussian Noise (AWGN) is symbolized by $w(n)$. The channel coefficient is given as $h(n)$ that can be further decomposed as:

$$h(n) = g(n).\xi(n), \quad (30)$$

In equation 30, $g(n)$ expresses zero-mean and single variance *i.i.d* channel coefficients, and the path loss component is shown by $\xi(n)$. Finally, from equation 30 the signal-to-noise ratio and distortion ratio (SDNR) can be derived as follows:

$$y = \frac{p\xi^2(n)E\left[|\alpha.x(n)|^2\right]}{p\xi^2(n)E\left[|d(n)|^2\right] + E\left(|w(n)|^2\right)} \quad (31)$$

The estimated obtainable ratio can be given as:

$$SE \approx K.E[\log_2(1+y)], \quad (32)$$

Here, the value of K is equal to $\left(\frac{T_{sl} - T_p}{T_{sl}}\right) \cdot \left(\frac{T_u}{T_s}\right)$ representing the scaling factor for the overhead of the pilot and the guard interval.

$$EE = \frac{k.E[\log_2(1+y)]}{(P_{pa} + P_i)} \quad (33)$$

In this article, we will employ equation 33 as a performance metric for the analysis. In functional and real conditions to obtain the best SNR performance without adding the proposed LSTM-NN reduction algorithm and for the case of adding the proposed method, it must utilize more expensive devices to give out the power compared with the latter. For instance, the SNR without adding the proposed scheme can be expressed as

$$SNR^{no} = p_{tx}^{no} \cdot \frac{1}{N_0 B} = \frac{p_{pa}^{no}}{\eta^{no}} \cdot \frac{1}{N_0 B} \quad (34)$$

In the above equation, the power of TX is denoted by p_{tx}^{no} . The power consumption is given p_{pa}^{no} . The efficiency of PA is illustrated as η^{no} in the case of the general OFDM system. For the given bandwidth the noise power is expressed as $N_0 B$. Finally, the SNR in the proposed method is represented as:

$$SNR^p = p_{tx}^p \cdot \frac{1}{N_0 B} = \frac{p_{pa}^p}{\eta^p} \cdot \frac{1}{N_0 B} \quad (35)$$

Here, p_{tx}^p shows the power of TX, similarly, the power consumption is expressed as p_{pa}^p , η^p shows the power efficiency of the proposed method. If $SNR^{no} = SNR^p$, it is clear that the value of p_{pa}^{no} should be larger than p_{pa}^p (i.e., $p_{pa}^{no} > p_{pa}^p$). It is because the efficiency of the traditional method is less than that of the proposed LSTM-NN scheme ($\eta^{no} < \eta^p$). We have added these parameters to the formula of the EE equation. And the computational complexity of the proposed is also shown in the same equation.

5. Simulation Results with Data Transmission

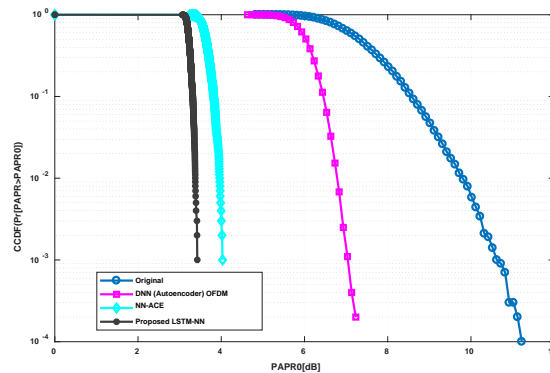
In this section, the simulation is performed for the proposed LSTM-NN method. The transmission of real-time data is compulsory for UAC to design novel methodologies and signal processing techniques. Therefore, we transmitted a WAV file in the simulation and kept the signal-to-noise ratio between 20-25dB. The simulation was performed on MATLAB 2017a adopting 16-QAM modulation. Firstly, we measured the PAPR and then compared it with traditional methods, besides that the channel impulse response (CIR) and sound speed are also measured in the initial stages. Next, we considered different parameters to verify the performance of the proposed method such as signal constellation points at the receiver side with BER. Finally, the relative energy analysis is illustrated. The simulation parameters are given in the following [Table 2](#).

Table 2. The UAC OFDM system Simulation Data

Serial No.	Parameter	Data
01	Sampling frequency	48 kHz
02	Bandwidth	6 -12 kHz
03	No. of Subcarriers	512
04	Number of data carriers	851
05	Number of pilots	125
06	Number of Null carriers	48
07	Symbol period	170.67ms
08	CP length	40ms
09	Spectrum Usage	0.67 b/s/Hz
10	Data rate	4.04 kb/s

5.1 Signal Transmission and PAPR

This subsection is dedicated to the transmission of data from the UAC transducer. The parameters such as PAPR and transmission of the signal before and after are being taken into consideration. In Fig. 5 the complementary cumulative distribution function (CCDF) of PAPR is depicted at 10^{-4} , the PAPR of the original signal is approximately 11.6 dB which can be seen in the blue curve. We compared the PAPR performance of deep learning neural network (DNN) auto-encoder-assisted OFDM and neural network-assisted active constellation (NN-ACE) with our proposed model, as shown in the magenta and cyan curve the PAPR of DNN auto-encoder OFDM and NN-ACE is around 6.8 dB and 4 dB, respectively. After comparison one can observe that the proposed LSTM-NN outperforms the conventional methods. The PAPR is reduced to 3.8 dB. Hence, efficient performance can be observed for PAPR in the LSTM-NN method.

**Fig. 5.** PAPR comparison of proposed with DNN (Autoencoder) and NN-ACE

The signal faces severe distortion which is caused by PA in the communication system. In the 16-QAM constellation, the OFDM symbols are shaped, and one can see the transmission of data before and after the PA at the transmission side as shown in Fig. 6. The non-linear distortion is extensively reduced in the LSTM-NN based method because the data is processed and filtered in the projected network. We kept sure that the PA is operating in the linear region, if the PA is not working in the linear region, it will distort the signal, so we have taken a 4dB value of the PA saturation level.

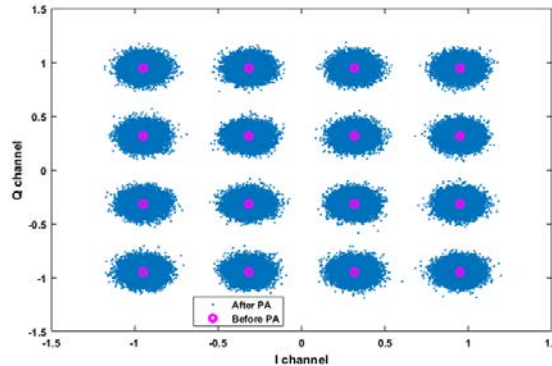


Fig. 6. Signal constellations, scattering plot before and after the power amplifier

5.2 Underwater Acoustic Channel Impulse Response with Sound Speed

In this part, the details about the experiment are given such as depth, separation, and position of the transmitter and receiver. The impulse response of the channel with a sound speed profile is executed for evaluating the performance of the proposed method. Fig. 7 illustrates the basic framework of the UAC system with a single transmitter (TX) and single receiver (RX). In the figure, P_{sb} exhibits the route between TX and RX having s surface and b bottom reflections. Five different paths can be observed in the figure, for instance, the signal's reflection from the surface only P_{10} reflected from the seabed P_{01} , and bounced from both the surface and bottom P_{11} , P_{12} including the direct path P_{00} which is considered the shortest path between the TX and the RX. Furthermore, L shows the distance between the transmitter and receiver, which is 2km. The transducer is dipped 12m in the water and the depth of the hydrophone is 14m.

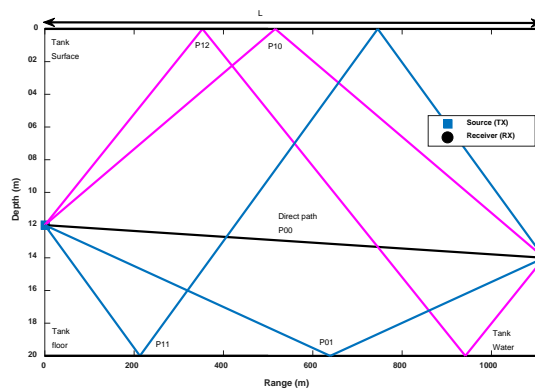


Fig. 7. UAC using the Bellhop ray-tracing model with a single transmitter & receiver.

The underwater acoustic channel has been established based on the BELLHOP ray-tracing model[2, 40]. The channel impulse response is measured from the sound speed as shown in Fig. 8, several multipath and delayed arrivals can be observed which is due to tank surface reflection, tank bottom reflection, and both, also rebounds from the walls. The sound speed profile which is shown in Fig. 9 was measured in an underwater acoustic water tank at Harbin engineering university during experimentation on October 25, 2020. As we mentioned earlier, the data from an experiment has been utilized to get the optimum results and for simulation purposes to design a novel signal processing methodology.

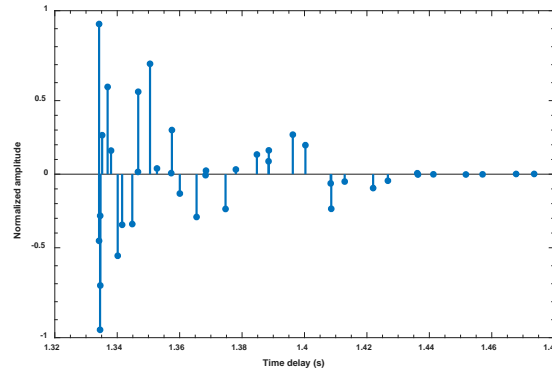


Fig. 8. Channel impulse response at 2KM between TX & RX

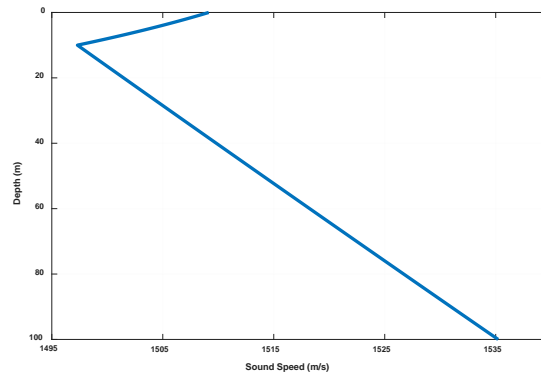


Fig. 9. Sound speed in the water measured during the experiment

5.3 Signal Reception and Bit Error rate

The signal reception and BER are studied in this sub-section. After the estimation of the channel, the decoder uses the information of output and of the channel equalizer to perform decoding based on LSTM-NN and updates the posterior probability of decoded symbol information where also our proposed algorithm is employed. **Fig. 10** depicts the data received from the hydrophone using the 16-QAM constellation at 25 dB SNR. The received data is much scattered out from the QAM quadrature because of the noisy multipath UAC channel, and the Doppler effect with spreading. While comparing **Fig. 10** and **Fig. 6** (subsection 5.1) one can see the impact of different parameters affecting the UAC channel which makes it a more challenging task in UAC. Although in our proposed model, the data is much nearer to the constellation, so we can demodulate it very easily. **Fig. 11** represents the BER of the communication system in the BELLHOP channel using 16-QAM. The curves represent the different neural network methods with proposed and conventional schemes. It can be observed from the figure that the proposed LSTM-NN achieves efficient BER performance over the traditional OFDM signal. Also, the performance is compared with DNN (Auto-encoder) and NN-ACE.

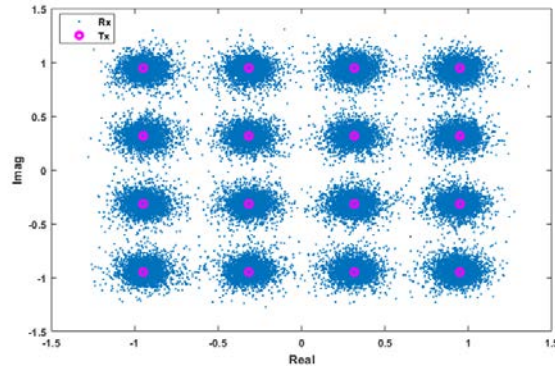


Fig. 10. Signal constellations, scattering plot of transmitted (TX) and received symbols (RX)

Fig. 12 illustrates the performance comparison of BER after using the OFDM modulation scheme at different types of constellations such as QPSK, 16-QAM, and 64-QAM, respectively. The black lines in the figure represent the QPSK constellation, one for simulation and another for real data transmission. It can be seen that there is a slight difference between the lines of QPSK when we transmit the real data at an SNR range of 25-30dB. The same SNRs are taken for the 16-QAM constellation having magenta curves. Also, a small difference is observed when we compare the simulations with the real transmission of data. In the end, for 64-QAM, we have shown in the blue curves, the range of SNRs is similar to that of QPSK. The obtained results show that the 64-QAM constellation has higher BER as compared to its counterparts. Here, we have employed 16-QAM for UAC, as it can provide us with significant gains and benefits for data transmission. The 64-QAM is a higher-order form of constellation type which carries extra bits of information per symbol, and it has a slightly higher BER. In the figure, the QPSK outperforms the rest of the schemes. The QPSK lashes the rest of the constellation schemes due to the small margin of bits transmitted through it.

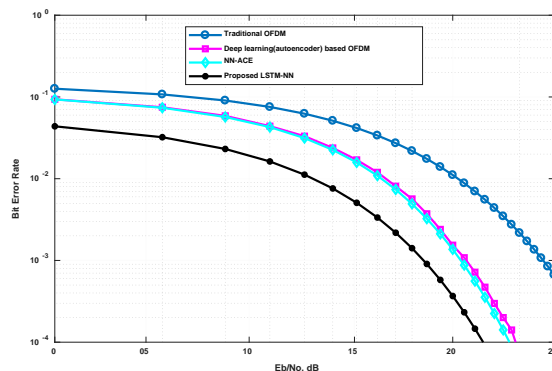


Fig. 11. Comparison of bit error rate with proposed LSTM-NN, DNN (Autoencoder) based OFDM and NN-ACE

5.3 Energy Efficiency Comparison

In **Fig. 13**, we have presented the EE comparison of different PAPR reduction schemes. The DNN (autoencoder) and NN-ACE are also shown in the figure with the proposed LSTM-NN model. The appropriate IBO (input back-off) is applied which is based on the performance of

PAPR reduction when the CCDF of PAPR is equal to 10^{-4} as shown in Fig. 5 (section 5.1). The EE depends upon the performance of PAPR in this model. When the SNR is equal to 30dB it shows the best performance, and the proposed model is applied. If the SNR is higher than 30dB we can get better performance in terms of EE because the proposed model reduces the PAPR at higher SNR. Hence it is proved that our proposed model gives us the improved performance of the overall system and the system can be regarded as energy efficient. The proposed method gives us the optimum performance of EE for all the SNR regions when compared with other PAPR reduction methods.

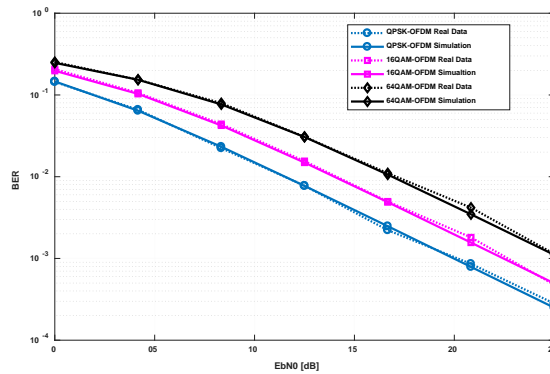


Fig. 12. BER performance of OFDM system over BELLHOP channel in UAC using a different type of constellations

6. Conclusions and Future Work

The OFDM is considered as significant modulation technique in the UAC system. The slow speed of sound, limited bandwidth, severe multipath, high Doppler shifts, and EE makes UAC more challenging. This paper proposed a machine learning-assisted LSTM-NN for the underwater acoustic OFDM communication system. The PAPR and nonlinear distortion are reduced with the proposed machine learning method, then different parameters are taken into consideration which affects the performance of the overall communication system to increase the EE. The real-time data is transmitted through the BELLHOP channel model by performing simulations. It is proved that our proposed LSTM-NN performs efficiently as compared to conventional DNN-based autoencoder and NN-ACE. Finally, the transmitted and received data is shown in the 16-QAM quadrature which proves that most of the data is close to the quadrature and can be demodulated and decoded easily. Also, the BER performs well for the LSTM-NN. By using this technique one can design a novel UAC modem/transceiver that will be energy efficient, and it will work proficiently. In future work, the Doppler compensation and time-varying nature of the UAC channel can be considered as an optimal research direction for the proposed method. Another potential research opportunity is an exhaustive search algorithm to perform optimal encoding and decoding order based on LSTM-NN which can omit the need for channel equalization, synchronization of the carrier frequency, modulation, and demodulation. The proposed system consists of a single transmitter and single receiver one can also implement our model to design an underwater acoustic wireless sensor network.

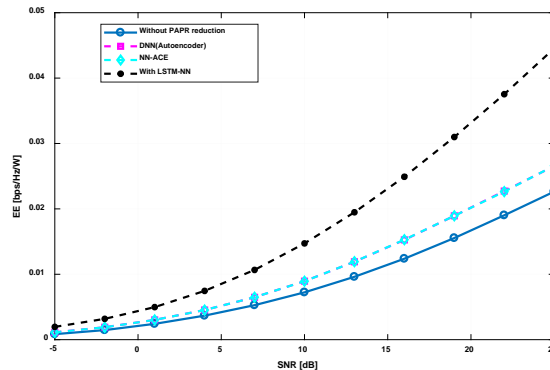


Fig. 13. Energy efficiency (bps/Hz/W) Vs. SNR [dB] with LSTM-NN, DNN(Autoencoder), NN-ACE scheme, and without PAPR reduction

Acknowledgment

The work was funded by the National Key Research and Development Program (No. 2022YFE0136800) and the Key Research and Autonomous Region of Key Research and Development Program of Tibet, China (No. XZ202101ZY0001F) including Research on Underwater Target Detection Based on Distributed MIMO (Ocean Defense Innovation Fund), and National Science and Technology Park of Harbin Engineering University.

References

- [1] B. Li, S. Zhou, M. Stojanovic, L. Freitag, and P. Willett, "Multicarrier Communication Over Underwater Acoustic Channels With Nonuniform Doppler Shifts," *IEEE Journal of Oceanic Engineering*, vol. 33, no. 2, pp. 198-209, 2008. [Article \(CrossRef Link\)](#).
- [2] James Preisig, Milica Stojanovic, "Underwater Acoustic Communication Channels: Propagation Models and Statistical Characterization," *IEEE Communications Magazine*, vol. 47, no. 1, pp. 84-89, 2009. [Article \(CrossRef Link\)](#)
- [3] D. Lucani, M. Medard, and M. Stojanovic, "Underwater Acoustic Networks: Channel Models and Network Coding Based Lower Bound to Transmission Power for Multicast," *IEEE Journal on Selected Areas in Communications*, vol. 26, no. 9, pp. 1708-1719, 2008. [Article \(CrossRef Link\)](#).
- [4] J.-g. Huang, H. Wang, C.-b. He, Q.-f. Zhang, and L.-y. Jing, "Underwater acoustic communication and the general performance evaluation criteria," *Frontiers of Information Technology & Electronic Engineering*, vol. 19, no. 8, pp. 951-971, 2018. [Article \(CrossRef Link\)](#).
- [5] J. A. C. Bingham, "Multicarrier modulation for data transmission: an idea whose time has come," *IEEE Communications Magazine*, vol. 28, no. 5, pp. 5-14, 1990. [Article \(CrossRef Link\)](#).
- [6] E. Bejjani and J. Belfiore, "Multicarrier coherent communications for the underwater acoustic channel," in *Proc. of OCEANS 96 MTS/IEEE Conference Proceedings. The Coastal Ocean - Prospects for the 21st Century*, vol. 3, pp. 1125-1130, 1996. [Article \(CrossRef Link\)](#).
- [7] G. Qiao, M. Muzzammil, N. Ahmed, and I. Ullah, "Experimental Investigation of Optimal Relay Position for Magneto-Inductive Wireless Sensor Networks," *Sensors*, vol. 20, 2020. [Article \(CrossRef Link\)](#).
- [8] M. Muzzammil, N. Ahmed, G. Qiao, I. Khan, and L. Wan, "Fundamentals and Advancements of Magnetic Field Communication for Underwater Wireless Sensor Networks," *IEEE Transactions on Antennas and Propagation*, vol. 68, no. 11, pp. 7555-7570, 2020. [Article \(CrossRef Link\)](#).

- [9] T. Xu and L. Xu, "Chapter 1 - Introduction," in *Digital Underwater Acoustic Communications*, T. Xu and L. Xu Eds. New York, NY, USA: Academic Press, pp. 1-30, 2017. [Article \(CrossRef Link\)](#)
- [10] Tianzeng Xu, Lufen Xu, *Digital Underwater Acoustic Communications*, 1st Edition, China Ocean Press. by Elsevier Inc.: Glyn Jones, 2017. [Article \(CrossRef Link\)](#)
- [11] Waleed Raza, Xuefei Ma, Amir Ali, Zubair Ali Shah & Ghazanfar Mehdi, "An Implementation of Partial Transmit Sequences to Design Energy Efficient Underwater Acoustic OFDM Communication System," *International Journal of Computer Science and Information Security (IJCSIS)*, Vol. 18, No. 4, pp. 19-26, 2020. [Article \(CrossRef Link\)](#)
- [12] Shengli Zhou, Zhaohui Wang, *OFDM for Underwater Acoustic Communications (Communication Technology)*, United States(US): Wiley Publishing, John Wiley & Sons, Ltd., June 2014, pp. 1-22. [Article \(CrossRef Link\)](#)
- [13] K. Byung-Chul and I. T. Lu, "Parameter study of OFDM underwater communications system," in *Proc. of OCEANS 2000 MTS/IEEE Conference and Exhibition. Conference Proceedings(Cat. No.00CH37158)*, vol. 2, pp. 1251-1255, 11-14 Sept. 2000. [Article \(CrossRef Link\)](#).
- [14] J. Allen and D. Berkley, "Image method for efficiently simulating small-room acoustics," *The Journal of the Acoustical Society of America*, vol. 65, pp. 943-950, 04/01 1979. [Article \(CrossRef Link\)](#).
- [15] Jurong Bai, Chenfei Cao, Yi Yang, Feng Zhao, Xiangjun Xin, Abdel-Hamid Soliman, Jiamin Gong, "Peak-to-average power ratio reduction for DCO-OFDM underwater optical wireless communication system based on an interleaving technique," *Optical Engineering*, vol. 57, no. 8, Paper 180820, 2018. [Article \(CrossRef Link\)](#).
- [16] D. R. K M, S.-H. Yum, E. Ko, S.-Y. Shin, J.-I. Namgung, and S.-H. Park, "Multi-Media and Multi-Band Based Adaptation Layer Techniques for Underwater Sensor Networks," *Applied Sciences*, vol. 9, no. 15, 2019. [Article \(CrossRef Link\)](#).
- [17] Jinqiu Wu, Gang Qiao, and Xiaofei Qi, "The Research on Improved Companding Transformation for Reducing PAPR in Underwater Acoustic OFDM Communication System," *Discrete Dynamics in Nature and Society*, 2016, Article ID 3167483. [Article \(CrossRef Link\)](#).
- [18] Jinqiu Wu, Xuefei Ma, Xiaofei Qi, Zeeshan Babar, and Wenting Zheng, "Influence of Pulse Shaping Filters on PAPR Performance of Underwater 5G Communication System Technique: GFDM," *Wireless Communications and Mobile Computing*, Vol. 2017, 2017, Article ID 4361589. [Article \(CrossRef Link\)](#).
- [19] D. Agarwal, N. Sharan, M. P. Raja, and A. Agarwal, "PAPR reduction using precoding and companding techniques for OFDM systems," in *Proc. of 2015 International Conference on Advances in Computer Engineering and Applications*, pp. 18-23, 19-20 March 2015. [Article \(CrossRef Link\)](#).
- [20] Aldo N. D' Andrea, V. Lottici and Ruggero Reggiannini, "RF Power Amplifier Linearization Through Amplitude and Phase Predistortion," *IEEE TRANSACTIONS ON COMMUNICATIONS*, vol. 44, No 11, pp. 1477-1484, 1996. [Article \(CrossRef Link\)](#).
- [21] X. Ma, W. Raza, Z. Wu, M. Bilal, Z. Zhou, and A. Ali, "A Nonlinear Distortion Removal Based on Deep Neural Network for Underwater Acoustic OFDM Communication with the Mitigation of Peak to Average Power Ratio," *Applied Sciences*, vol. 10, no. 14, 2020. [Article \(CrossRef Link\)](#).
- [22] S. Xing, G. Qiao, and L. Ma, "A Blind Side Information Detection Method for Partial Transmitted Sequence Peak-to-Average Power Reduction Scheme in OFDM Underwater Acoustic Communication System," *IEEE Access*, vol. 6, pp. 24128-24136, 2018. [Article \(CrossRef Link\)](#).
- [23] J. Tellado, L. M. C. Hoo, and J. M. Cioffi, "Maximum-likelihood detection of nonlinearly distorted multicarrier symbols by iterative decoding," *IEEE Transactions on Communications*, vol. 51, no. 2, pp. 218-228, 2003. [Article \(CrossRef Link\)](#).
- [24] F. H. Gregorio, S. Werner, J. Cousseau, J. Figueroa, and R. Wichman, "Receiver-side nonlinearities mitigation using an extended iterative decision-based technique," *Signal Processing*, vol. 91, no. 8, pp. 2042-2056, 2011. [Article \(CrossRef Link\)](#).

- [25] M. Kim, W. Lee, and D.-H. Cho, "A Novel PAPR Reduction Scheme for OFDM System Based on Deep Learning," *IEEE Communications Letters*, vol. 22, no. 3, pp. 510-513, 2018. [Article \(CrossRef Link\)](#).
- [26] M. Kim, W. Lee, J. Yoon, and O. Jo, "Toward the Realization of Encoder and Decoder Using Deep Neural Networks," *IEEE Communications Magazine*, vol. 57, no. 5, pp. 57-63, 2019. [Article \(CrossRef Link\)](#).
- [27] Y. Zhang, J. Li, Y. Zakharov, X. Li, and J. Li, "Deep learning based underwater acoustic OFDM communications," *Applied Acoustics*, vol. 154, pp. 53-58, 2019. [Article \(CrossRef Link\)](#).
- [28] A. N. H. a., T. Shongwe, "Proposed Machine Learning System to Predict and Estimate Impulse Noise in OFDM Communication System," in *Proc. of the IECON 2016 - 42nd Annual Conference of the IEEE Industrial Electronics Society*, 2016. [Article \(CrossRef Link\)](#)
- [29] H. Ye, G. Y. Li, and B.-H. Juang, "Power of Deep Learning for Channel Estimation and Signal Detection in OFDM Systems," *IEEE Wireless Communications Letters*, vol. 7, no. 1, pp. 114-117, 2018. [Article \(CrossRef Link\)](#).
- [30] Tomohisa Wada, Takao Toma, Mursal Dawodi and Jawid Baktash, "A Denoising Autoencoder based wireless channel transfer function estimator for OFDM communication system," in *Proc. of the 2019 International Conference on Artificial Intelligence in Information and Communication (ICAIIIC)*, Okinawa, Japan, 2019. [Article \(CrossRef Link\)](#)
- [31] Mingshan Zhang, Ming Liu and Zhangdui Zhong, "Neural Network Assisted Active Constellation Extension for PAPR Reduction of OFDM System," in *Proc. of the 11th International Conference on Wireless Communications and Signal Processing (WCSP)*, Xi'an, China, Xi'an, China, 2019. [Article \(CrossRef Link\)](#)
- [32] Lanping Li, Chintha Tellambura and Xiaohu Tang, "Improved Tone Reservation Method Based on Deep Learning for PAPR Reduction in OFDM System," in *Proc. of the 2019 11th International Conference on Wireless Communications and Signal Processing (WCSP)*, Xi'an, China, 2019. [Article \(CrossRef Link\)](#)
- [33] M. S. El-Mahallawy, E. A. A. Hagrass, and S. A. Fathy, "Genetic algorithm for PAPR reduction in SLM wavelet-OFDM systems," in *Proc. of 2014 International Conference on Computer, Control, Informatics and Its Applications (IC3INA)*, pp. 136-140, 2014. [Article \(CrossRef Link\)](#).
- [34] M. Lixia, M. Murrioni, and V. Popescu, "PAPR reduction in multicarrier modulations using Genetic Algorithms," in *Proc. of 2010 12th International Conference on Optimization of Electrical and Electronic Equipment*, pp. 938-942, 2010. [Article \(CrossRef Link\)](#).
- [35] Y. Wang, W. Chen, and C. Tellambura, "Genetic Algorithm Based Nearly Optimal Peak Reduction Tone Set Selection for Adaptive Amplitude Clipping PAPR Reduction," *IEEE Transactions on Broadcasting*, vol. 58, no. 3, pp. 462-471, 2012. [Article \(CrossRef Link\)](#).
- [36] M. Hosseinzadeh Aghdam and A. A. Sharifi, "PAPR reduction in OFDM systems: An efficient PTS approach based on particle swarm optimization," *ICT Express*, vol. 5, no. 3, pp. 178-181, 2019. [Article \(CrossRef Link\)](#).
- [37] A. A. Parandoosh, J. Taghipour, and V. T. Vakili, "A Novel Particle Swarm Optimization for PAPR Reduction of OFDM Systems," in *Proc. of the 2012 International Conference on Control Engineering and Communication Technology*, 2012. [Article \(CrossRef Link\)](#)
- [38] I. Sohn, "A Low Complexity PAPR Reduction Scheme for OFDM Systems via Neural Networks," *IEEE Communications Letters*, vol. 18, no. 2, pp. 225-228, 2014. [Article \(CrossRef Link\)](#).
- [39] T. Tabbat and E. Panayirci, "Channel Estimation and Equalization Algorithm for OFDM-Based Underwater Acoustic Communications Systems," in *Proc. of The Thirteenth International Conference on Wireless and Mobile Communications*, pp. 113-118, 2017. [Article \(CrossRef Link\)](#).
- [40] Y. Zhang et al., "Deep Learning Based Single Carrier Communications Over Time-Varying Underwater Acoustic Channel," *IEEE Access*, vol. 7, pp. 38420-38430, 2019. [Article \(CrossRef Link\)](#).
- [41] J. Zhang, Y. Cao, G. Han, and X. Fu, "Deep neural network-based underwater OFDM receiver," *IET Communications*, vol. 13, no. 13, pp. 1998-2002, 2019. [Article \(CrossRef Link\)](#).

- [42] L. Hao, D. Wang, Y. Tao, W. Cheng, J. Li, and Z. Liu, "The Extended SLM Combined Autoencoder of the PAPR Reduction Scheme in DCO-OFDM Systems," *Applied Sciences*, vol. 9, no. 5, 2019. [Article \(CrossRef Link\)](#).
- [43] R. M. G. a. J. M. L. Manickam, "PAPR Reduction Technique Using Combined DCT and LDPC based OFDM system for Underwater Acoustic Communication," *ARN Journal of Engineering and Applied Sciences*, vol. 11, pp. 4424-4430, 2016. [Article \(CrossRef Link\)](#).
- [44] M. Stojanovic, "OFDM for underwater acoustic communications: Adaptive synchronization and sparse channel estimation," in *Proc. of 2008 IEEE International Conference on Acoustics, Speech and Signal Processing*, pp. 5288-5291, 31 March-4 April 2008. [Article \(CrossRef Link\)](#).
- [45] Y. V. Zakharov and V. P. Kodanov, "Multipath-Doppler diversity of OFDM signals in an underwater acoustic channel," in *Proc. of 2000 IEEE International Conference on Acoustics, Speech, and Signal Processing. Proceedings (Cat. No.00CH37100)*, vol. 5, pp. 2941-2944, 2000. [Article \(CrossRef Link\)](#).
- [46] Y. V. Zakharov and A. K. Morozov, "OFDM Transmission Without Guard Interval in Fast-Varying Underwater Acoustic Channels," *IEEE Journal of Oceanic Engineering*, vol. 40, no. 1, pp. 144-158, 2015. [Article \(CrossRef Link\)](#).
- [47] B. M. Lee, Y. S. Rim, and W. Noh, "A combination of selected mapping and clipping to increase energy efficiency of OFDM systems," *PLoS One*, vol. 12, no. 10, p. e0185965, 2017. [Article \(CrossRef Link\)](#)
- [48] Sroy Abouty, Li Renfa, Zeng Fanzi and Fall Mangone, "A Novel Iterative Clipping and Filtering Technique for PAPR Reduction of OFDM Signals: System Using DCT/IDCT Transform," *International Journal of Future Generation Communication and Networking*, Vol. 6, no. 1, pp. 1-8, 2013. [Article \(CrossRef Link\)](#).
- [49] A. Graves, *Supervised Sequence Labelling with Recurrent Neural Networks*, 2012. [Article \(CrossRef Link\)](#)
- [50] Hochreiter Sepp and Jürgen Schmidhuber, "Long Short-term Memory," *Neural computation*, vol. 9, pp. 1735-1780, 12/01 1997. [Article \(CrossRef Link\)](#)



Waleed Raza received a B.E. degree in Electronic Engineering from the Department of Electronic Engineering, Dawood University of Engineering and Technology Karachi, Pakistan in 2017. He has received an M.S. degree in underwater acoustic communication engineering from the College of Underwater Acoustic Engineering, Harbin Engineering University, Harbin China where he published several research articles in the OFDM communication for underwater technology. He holds the Editorial Board Member for Engineering, Technology, and Applied Science Research (ETASR) (2021-present), He is an Active Reviewer of a few journals including IEEE Sensor Journal, IEEE Access, and International Journal of Electronics and Communications (2018-2022), he has joined the IEEE as a student member. Currently, he is pursuing a Ph.D. degree at Embry Riddle Aeronautical University in Electrical and Computer Engineering. His research area of interest includes underwater acoustic OFDM communication, underwater acoustic target detection, Artificial Intelligence, Machine Learning for Communication Engineering, Autonomous Unmanned Systems such as UAVs and their characteristics.



Xuefei Ma received the B.S. degree in electronic information engineering from the Harbin Engineering University, China, in 2003, the M.S. degree in information and communication engineering from the Harbin Engineering University, China, in 2006, and the Ph.D. degree in Signal and information processing engineering from the college of Information and Communication Engineering, Harbin Engineering University, China, in 2011, where he is currently a professor. He has authored more than ten papers in SCI and EI, among which the first author and the author of the communication published eight SCI papers. He has received 22 invention patents. His main research interests are underwater acoustic communication technology, underwater acoustic detection, and guidance technology. Dr. Ma is an Editor-in-Chief of the 13th Five-Year key planning book The Principles and Applications of Electronic Measuring Instruments, and the Deputy Editor of Twelfth Five-Year National Key Book Planning Project and Academic Monograph of National Defense Characteristics Textbook Satellite Navigation Principle. His research interests include underwater acoustic detection, underwater acoustic communication, and underwater acoustic localization.



Houbing Song (M'12–SM'14–F'23) received the Ph.D. degree in electrical engineering from the University of Virginia, Charlottesville, VA, in August 2012. He is currently a Tenured Associate Professor and the Director of the Security and Optimization for Networked Globe Laboratory (SONG Lab, www.SONGLab.us), University of Maryland, Baltimore County (UMBC), Baltimore, MD. Prior to joining UMBC, he was a Tenured Associate Professor of Electrical Engineering and Computer Science at Embry-Riddle Aeronautical University, Daytona Beach, FL. He serves as an Associate Editor for IEEE Transactions on Artificial Intelligence (TAI) (2023-present), IEEE Internet of Things Journal (2020-present), IEEE Transactions on Intelligent Transportation Systems (2021-present), and IEEE Journal on Miniaturization for Air and Space Systems (J-MASS) (2020-present). He was an Associate Technical Editor for IEEE Communications Magazine (2017-2020). He is the editor of eight books, the author of more than 100 articles and the inventor of 2 patents. His research interests include cyber-physical systems/internet of things, cybersecurity and privacy, and AI/machine learning/big data analytics. His research has been sponsored by federal agencies (including National Science Foundation, US Department of Transportation, and Federal Aviation Administration, among others) and industry. His research has been featured by popular news media outlets, including IEEE GlobalSpec's Engineering360, Association for Uncrewed Vehicle Systems International (AUVSI), Security Magazine, CXOTech Magazine, Fox News, U.S. News & World Report, The Washington Times, and New Atlas. Dr. Song is an IEEE Fellow, an ACM Distinguished Member, and an ACM Distinguished Speaker. Dr. Song is a Highly Cited Researcher identified by Clarivate™ (2021, 2022) and a Top 1000 Computer Scientist identified by Research.com. He received Research.com Rising Star of Science Award in 2022 (World Ranking: 82; US Ranking: 16). Dr. Song was a recipient of 10+ Best Paper Awards from major international conferences, including IEEE CPSCoM-2019, IEEE ICII 2019, IEEE/AIAA ICNS 2019, IEEE CBDCoM 2020, WASA 2020, AIAA/ IEEE DASC 2021, IEEE GLOBECOM 2021 and IEEE INFOCOM 2022.



Amir Ali received a B.E. degree in Electronic Engineering from the Department of Electronic Engineering, Mehran University of Engineering and Technology Jamshoro, Pakistan in 2016. He is currently pursuing an M.S. degree in Hydroacoustic engineering at the College of Underwater Acoustic Engineering, Harbin Engineering University, Harbin China. His research area of interest includes underwater acoustic communication.



Habib Hussain Zuberi received a B.E. degree in Electrical Engineering with a specialization in telecommunication engineering from the Department of Electrical Engineering, Bahria University Karachi, Pakistan in 2009, and an M. Eng. in telecommunication engineering from NED University of engineering and technology Karachi, Pakistan in 2013. He has been teaching at Bahria University Karachi campus since 2014. He is currently pursuing a Ph.D. degree in Information and Communication with the College of Underwater Acoustic Engineering, Harbin Engineering University, China. His research interests include underwater acoustic Communication and wireless communication.



Kamal Acharya is an experienced Information Technology Coordinator with a demonstrated history of working in the education management industry. He is skilled in PHP, C++, Meteor, jQuery, and Python. He has strong information technology professional with a Bachelor of Engineering (B.E.) degree focused on electronics and communication and a master's degree in information system engineering from the College of Applied Business, Katmandu, Nepal. Currently, he is pursuing a Ph.D. degree at Embry Riddle Aeronautical University. His research interests include cybersecurity and privacy, and AI/machine learning/big data analytics.